Int J Adv Manuf Technol (2015) 77:2051–2058
DOI 10.1007/s00170-014-6577-x

ORIGINAL ARTICLE

The effect of FSP on mechanical, tribological, and corrosion behavior of composite layer developed on magnesium AZ91 alloy surface

M. Abbasi · B. Bagheri · M. Dadaei · H. R. Omidvar · M. Rezaei

Received: 8 August 2014 / Accepted: 9 November 2014 / Published online: 27 November 2014

Abstract Friction stir processing (FSP) has been applied to modify the surface characteristics of metals. Development of surface composites through FSP has been addressed by different research studies. During the process, generally hard particles are embedded in the soft matrix through stirring. In the current research, surface composites were developed on the surface of AZ91 magnesium base alloy. SiC and Al_2O_3 particles were embedded separately in the surface and accordingly two kinds of composites were developed. Different characteristics, namely mechanical, tribological, and corrosion behavior, were analyzed. The results showed that mechanical properties as well as strength, hardness, and ductility of FS-processed samples were higher than the as-received one. It was concluded that wear and corrosion resistance of FS-processed samples were higher than the as-received material. The results also indicated that by increment of pass number, the mechanical properties improved, corrosion resistance increased, and wear rate decreased. The results also showed that samples processed using SiC particles had better mechanical characteristics and corrosion resistance than samples processed using Al_2O_3 particles, although particle type did not have significant effect on wear rate.

Keywords Friction stir processing · AZ91 magnesium alloy · Surface composite · Wear · Corrosion

M. Abbasi (✉)
Faculty of Engineering, University of Kashan, Kashan, Iran
e-mail: m.abbasi@aut.ac.ir

B. Bagheri · H. R. Omidvar · M. Rezaei
Department of Mining and Metallurgy,
Amirkabir University of Technology, Tehran, Iran

M. Dadaei
Chaharmahal Bakhtiari automotive sheet company,
Chaharmahal Bakhtiari, Iran

1 Introduction

Magnesium alloys, being among the lightest structural materials, are very attractive in industries. They are gaining importance as a structural material for applications in which weight reduction is crucial, due to their low density and high stiffness-to-weight ratio [1]. However, the mechanical properties, such as the hardness of the magnesium alloys, are not sufficient to enhance their applications. Some processes to fabricate ceramics particles/magnesium alloy composites have been studied to improve the mechanical properties [2]. Recently, friction stir processing (FSP) has been developed based on friction stir welding (FSW) for microstructure modification of the metals. FSW, which is a novel solid-state welding method, has increased the importance of welding technology especially for Al, Mg, and Cu alloys and stainless steels, which are difficult to weld through conventional welding methods. Review articles [3–5], addressing FSW/FSP, summarized different research studies done in this area. FSP has similarity with FSW, although it is used for processing of metal surface. By application of FSP, microstructural changes such as breakup of as-cast microstructure, grain refinement, homogenization of precipitates, and elimination of casting defects are expected [6]. Thus, FSP is believed to be one of the most useful methods for improving mechanical properties. It is possible to produce surface composite layer by this process as well [7]. FSP is a method of changing the properties of a metal surface through intense, localized plastic deformation. This deformation is produced by forcibly inserting a nonconsumable tool into the workpiece and revolving the tool in a stirring motion as it is pushed laterally through the workpiece [8].

AZ91 alloy is the most widely used magnesium alloy. AZ91 magnesium alloy is widely used in aerospace, automobile, and electronic industries due to its high castability, wide range of room temperature mechanical properties, and high corrosion resistance [9].

Asadi et al. [2] fabricated SiC/AZ91 composite layer using FSP. They studied the effect of process parameters such as rotational and traverse speeds, tool penetration depth, and tilt angle on the formation of defects such as cracks, tunneling cavity, and also on sticking of matrix material to tool. They also considered the effect of these parameters on the mechanical properties and microstructures of specimens. They found that FSP is an effective process to fabricate SiC/AZ91 composite layer with uniform distribution of SiC particles, good interfacial integrity, and significant grain refinement. They also concluded that the increase of the rotational and traverse speeds lead to a decrease in the grain size.

Arora et al. [10] improved the microhardness value of a magnesium alloy AE42 nearly by 60 % conducting FSP under rapid external cooling. Uematsu et al. [6] applied FSP to cast magnesium alloy AZ91-F to modify the as-cast microstructure. They studied fatigue behavior of as-cast, T5-aged, and their FS-processed specimens based on microstructural consideration, crack initiation, crack growth behavior, and fracture surface analysis. They found that FS-processed specimens exhibited significantly higher fatigue strength than the as-cast and T5-aged specimens. FSP resulted in the breakup of coarse as-cast microstructure, grain refinement of the matrix, finely dispersed precipitates, and increase of hardness. Both the crack initiation resistance and crack growth resistance considerably enhanced compared with the as-cast and T5-aged specimens, and fatigue strengths of the FS-processed specimens improved.

Singh et al. [1] fabricated an AZ91-based hybrid composite using FSP with TiC as reinforcement. FSP of AZ91 was conducted with particle addition under ambient cooling conditions. They studied wear behavior of fabricated nanocomposites using pin on disk wear test.

In the current research, composite layer was developed on the surface of magnesium AZ91 alloy using FSP. Two kinds of nanoparticles were used. SiC and Al_2O_3 particles were embedded separately in magnesium AZ91 alloy matrix and two surface composites, namely surface composite included SiC particles and surface composite included Al_2O_3 particles, were developed. Wear, corrosion resistance, and mechanical properties of processed materials were compared with the as-received material.

2 Materials and methods

2.1 As-received material

The material used in this research was AZ91 magnesium alloy in as-cast condition. Blanks 7 mm in thickness were prepared from the ingot, and these blanks were FS-processed. The chemical composition of the alloy is given in Table 1. α-Mg matrix and heterogeneously distributed second-phase β-$Mg_{17}Al_{12}$ particles along the grain boundaries characterize the as-received microstructure of the studied material. The as-received microstructure is presented in Fig. 1.

2.2 Friction stir processing

Grooves 2 mm in depth, 1 mm in width, and 130 mm in length were cut on the surfaces of AZ91 specimens. The groove was filled with reinforcing particles, and then, the tool was moved along the groove. The specimens were first processed using a tool which only consisted of shoulder without pin to seal the groove. FSP was then conducted with a tool consisting of shoulder and pin. Sealing inhibits the scattering of particles during FSP. Some specimens were processed using SiC particles, and some were processed using Al_2O_3 ones. The grooves were filled with the same content of particles, 0.63 g, with grain size of 30 nm. An image analyzer program was used to evaluate the size of grains.

Vertical milling machine was used to conduct friction stir processing. A simple FSP tool was used in this work; the tool was made of H-13 tool steel and consisted of a shoulder 15 mm in diameter and a pin 4 mm in diameter, 2.5 mm in height. Shoulder and pin had a cylindrical shape. The tool used for sealing had similar characteristics but without the pin. To get the optimum conditions of processing, several samples were FS-processed at different combinations of rotational (730–1800 rpm) and translational (14–80 mm min^{-1}) speeds based on research data reported in [11, 12]. The FSP tool was tilted by 2° from the workpiece normal axis, and a mixture of dry ice and ethanol was applied as coolant. Additionally, different pass numbers, 1–4 passes, were conducted in order to evaluate the effect of pass number on the properties of the specimens.

Specimens for tensile testing were cut from processed samples along the processing direction based on ASTM-E8 [13]. Tensile tests were carried out on a 50-kN, electromechanically controlled table-top tensometer.

Proper selection of FSP parameters, such as rotating speed, traverse speed, configuration of pin, and type of coolant, was carried out based on experimental investigations. More information about this data can be found in [14]. During the processing, rotational speed was 950 rpm, and traverse speed was 42 mm min^{-1}. The surface appearance of a FS-processed sample with optimized parameters is shown in Fig. 2.

Table 1 Chemical composition of the studied alloy

Element	A1	Zn	Mn	Si	Cu	Ni	Fe	Mg
Wt%	9.1	0.68	0.14	0.085	0.0097	0.001	0.0021	Balance

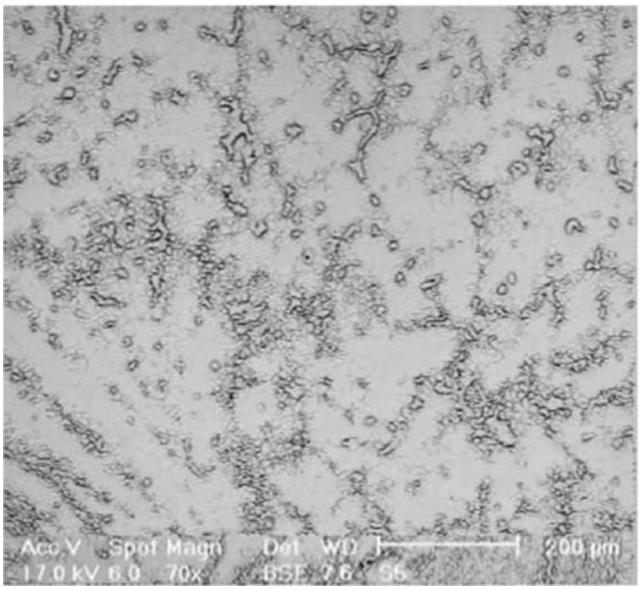

Fig. 1 The as-received microstructure of the studied alloy

2.3 Characterization of mechanical properties

Tensile test specimens were prepared based on the ASTM-E8 standard test [13] with a strain rate of 10^{-5} s^{-1}. The hardness was measured using a Vickers microhardness tester. The applied test load was 100 gf, and the dwell time was 10 s. The average of five readings for hardness within each tested area was calculated and reported.

2.4 Characterization of wear behavior

The wear testing based on ASTM G99 standard test [15] was conducted on TRI-PIN-ON-DISK equipment using a stainless steel 316 L (ASTM) disk as a counterface, in the presence of distilled water with a sliding speed of 1 mm s^{-1}, contact force of 50 N, and total distance of 500 m. Cylindrical pins with 5-mm diameter and 40-mm height were prepared from studied samples using wire cut. The counterface disks were prepared by polishing them in a polishing equipment using abrasive disks with 100, 200, 320, 400, 600, and 1200 mesh, in the sequence, under water circulation. The disks were washed, first with detergent and water and then with absolute ethyl alcohol. After that, the solvent was evaporated in hot air flow.

Fig. 2 The surface appearance of the FS-processed sample

2.5 Characterization of corrosion behavior

Specimens used for the electrochemical corrosion tests were mounted on FS-processed specimens with epoxy resin to give an exposed area of 1 cm^2. Before each test, the specimen was washed by acetone and distilled water and finally was used as working electrode. The experiments were conducted in a conventional three electrode electrochemical cell with a volume of 100 cm^3 at room temperature (~25 °C). Also, a platinum plate (2 cm^2) and an Ag|AgCl 3 M KCl (0.207 V vs SHE) were used as the counter and reference electrodes, respectively. The electrolyte was 3.5 wt% NaCl solution. The tests were performed at a scan rate of 1 mV s^{-1}. Tafel extrapolation analyses were performed under both anodic and cathodic conditions at OCP up to ±0.15 V under aerated conditions after an initial delay time of 400 s.

3 Results and discussion

3.1 Mechanical properties

3.1.1 Tensile test

Tensile strength and elongation values of the samples studied are given in Table 2. It can be seen from Table 2 that for all FS-processed samples, the strength and ductility values are higher than those for as-received sample. The tensile test results indicates that for one-pass processed sample, both strength and ductility values are lower than those for the FS-processed sample with no particle addition. This can be assigned to agglomeration and nonhomogeneous distribution of particles during one-pass processing which accelerate nucleation and growth of cracks during tensile test [16]. As can be seen in

Table 2 Comparison of mechanical properties relating to FS-processed samples and as-received sample

Sample	UTS (MPa)	Elongation (%)	FI (MPa %)
As-received	124.56	10.1	1258.84
FSP-No particle	203.65	14.04	2859.84
FSP-SiC			
One-pass	171.57	12	2058.84
Two-pass	306.63	13.05	4001.52
Four-pass	390.71	16.56	6470.15
FSP-SiC			
One-pass	155	11	1705
Two-pass	287.67	12.51	3598.75
Four-pass	372.96	16.05	5986

FI formability index

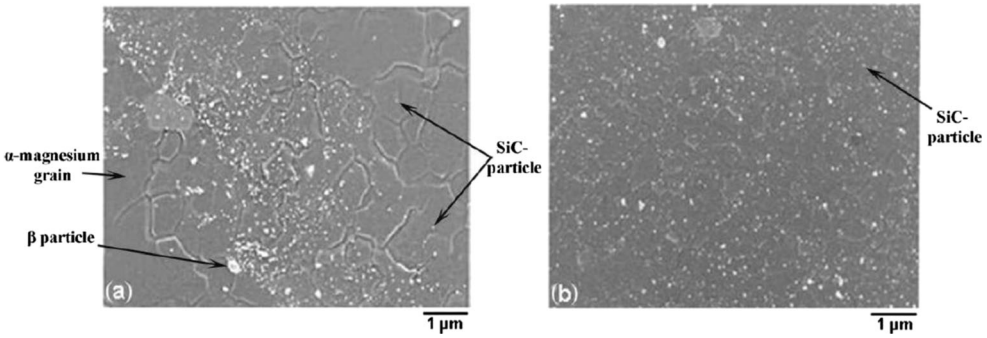

Fig. 3 SEM pictures of stirred zone related to FS-processed samples using SiC particles corresponding to different pass numbers: **a** 1 and **b** 4

Fig. 3, the increase of pass number during FSP results in more grain refinement and more homogeneous distribution of reinforcing particles which delay crack initiation and growth. So, increment of strength and ductility as pass number enhances is inevitable. An increase in mechanical properties through increasing pass numbers, due to the breakup of coarse dendrites, elimination of porosity, and refinement of matrix grains, has also been reported by other researchers [17, 18].

Moreover, the data in Table 2 reveals that FS-processed samples using SiC particles have higher strength and ductility values compared to samples processed using Al_2O_3 particles. Dadaei et al. [7] noted that SiC particles distribute homogeneously during FSP because of their characteristics, and as a result, crack nucleation and propagation are postponed.

Formability indices of studied samples are also compared in Table 2. The formability index, which is the ability of a material to have both a good ductility (A_{25}) or formability and a high strength (ultimate tensile strength (UTS)), is best quantified using the equation UTS$\times A_{25}$ [19]. It can be seen from Table 2 that formability indices of FS-processed samples are largely higher than those for as-received alloy; furthermore, it is concluded from Table 2 that by an increase in pass number, formability index increases. This can be related to the effect of FSP on strength and ductility values of the as-received material which enhances them and correspondingly improves the formability index. Moreover, the data in Table 2 also reveal that formability indices of FS-processed samples with SiC particles are higher than those processed with Al_2O_3 particles. As stated before, these phenomena result from high strength and ductility of SiC-processed samples compared to Al_2O_3-processed ones.

3.1.2 Hardness test

Hardness measurements were taken on transverse sections of FS-processed samples. Five measurements were taken for each sample and the mean value was calculated and reported. Measurements revealed that the hardness of the FS-processed sample was higher than that of the as-received sample. Enhancement of hardness represents an increase in the ability of substance to withstand the deformation [16]. Grain refinement and presence of second-phase particles in microstructure of FS-processed sample are the two main factors that limit the deformation. The smaller size of grains and second-phase particles result in higher hardness values [16, 17].

Hardness values of some FS-processed samples using SiC as well as Al_2O_3 particles for single pass and multipasses are presented in Fig. 4. It is observed that by increasing the number of passes, as grains size decreases and the distribution of second-phase particles improves, the hardness value increases.

3.2 Wear resistance

SEM pictures of worn surfaces relating to base material and one-pass processed samples are shown in Fig. 5. As it is observed in Fig. 5, grooves in base metal are deeper than those in processed samples. This can be related to the low hardness of as-received material in regard with those of

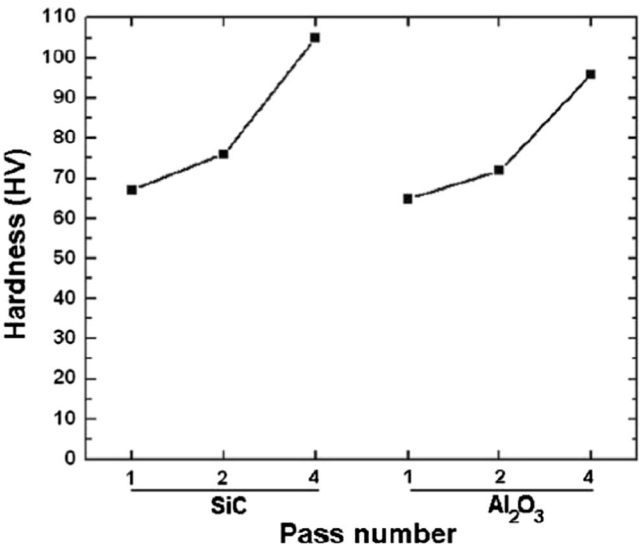

Fig. 4 The effect of pass number and reinforcing particle type on variation of hardness values for FS-processed samples

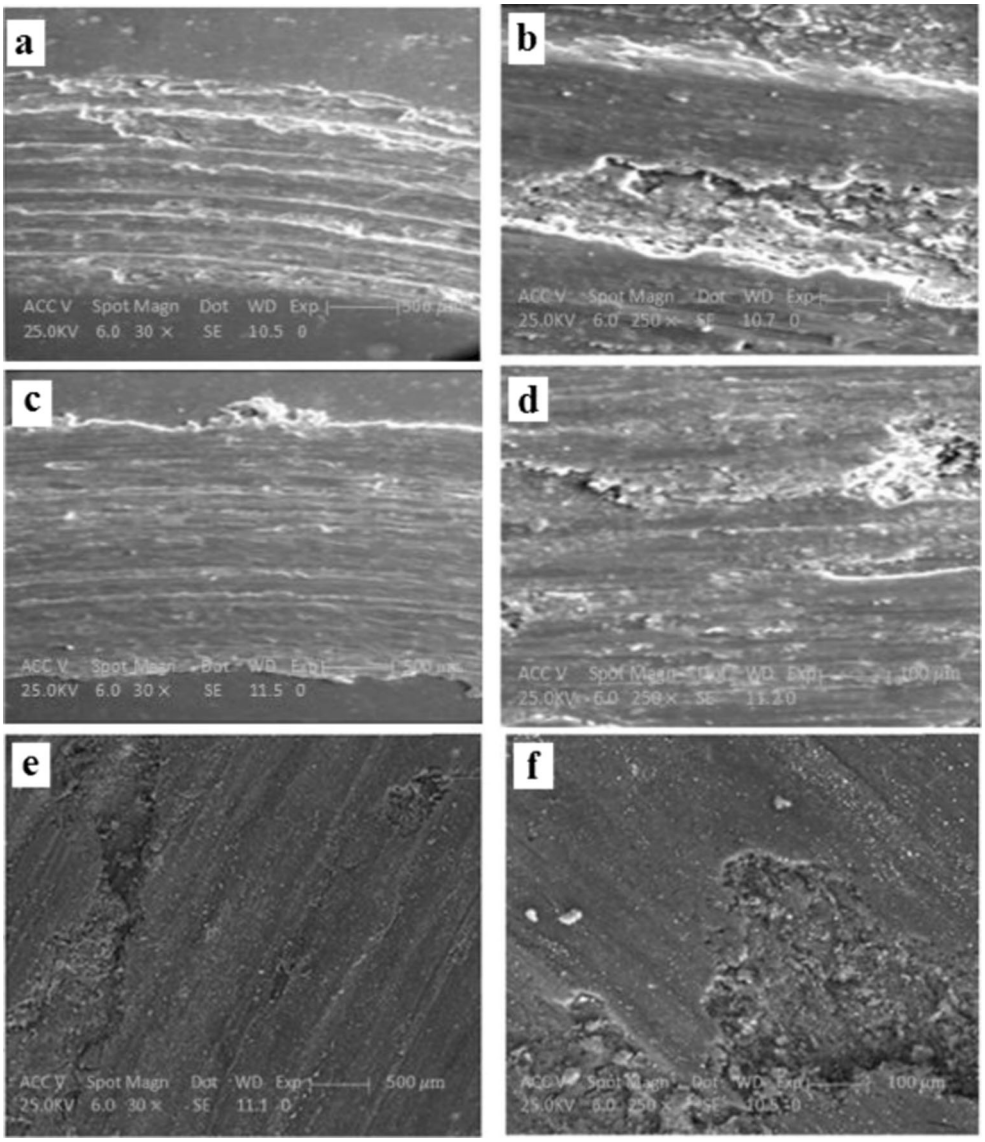

Fig. 5 Worn surfaces of base material (**a**, **b**) and FS-processed samples (**c**–**f**) after wear test (**c**, **d** relate to samples FS-processed with SiC particles while **e**, **f** relate to samples processed with Al_2O_3 particles)

processed samples. High hardness inhibits formation of deep grooves during wear.

Variation of friction coefficient as a function of sliding distance for base material and processed samples are shown in Fig. 6. Figure 6 shows that variation of friction coefficient for base metal is extensive, while these changes for processed samples are not extensive. As it is observed in Fig. 6, friction coefficient changes for four-pass processed samples is insignificant. These observations might be related to the effect of FSP on surface layer of the as-received material. By increment of pass number during FSP, surface microstructure is modified and more homogenous microstructure is obtained. Homogeneity prevents from large variation in friction coefficient.

High friction coefficient in some areas of base material as well as micrograph shown in Fig. 6 indicate that adhesive wear mechanism is dominant in base material. Furthermore, presence of scratches in wear surface of one-pass processed samples (Fig. 5) depict that abrasive wear mechanism is dominant.

According to Sarkar [20], abrasive wear occurs when either a rough, hard surface or a soft surface with hard particles embedded in its surface slides over a softer material. A plowing action takes place, and scratches or parallel furrows in the direction of motion form. Additionally, when two surfaces are brought together under load, asperities of the two surfaces adhere to each other and a bond is formed between asperities. During sliding, these junctions are sheared. This will result in adhesive wear in which a wear fragment is being transferred from one surface to the other [20].

Material transfer in some areas of one-pass processed sample can be related to weakness of material in these areas due to particle agglomeration. During wear test, material in weak regions is sheared and transforms.

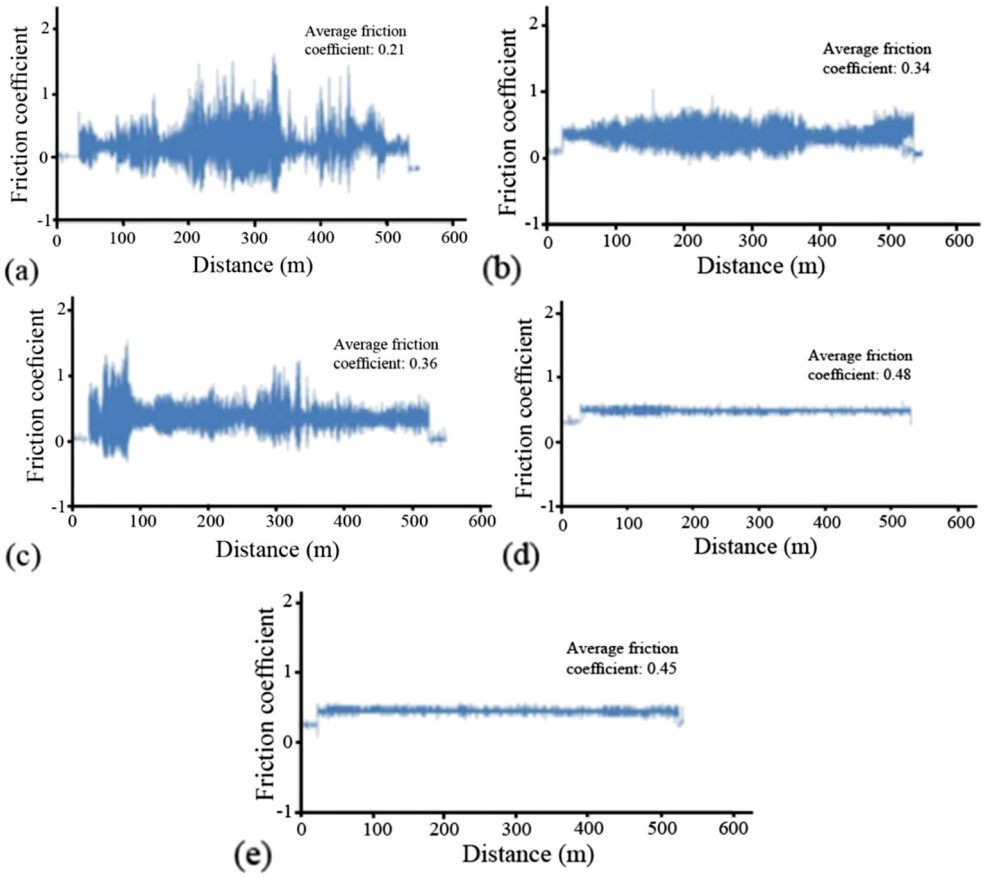

Fig. 6 Variation of friction coefficient as a function of sliding distance for base material as well as FS-processed samples (**a** relate to base material, **b**, **c** relate to one-pass FS-processed samples, and **d**, **e** relate to four-pass FS-processed samples; **b**, **d** relate to samples processed using SiC particles and **c**, **e** relate to samples processed with Al_2O_3 particles)

SEM pictures of worn surfaces relating to four-pass processed samples are presented in Fig. 7. Presence of parallel grooves which are indicators of abrasive wear mechanism are observable in Fig. 7. Friction coefficient measurements for these samples in Fig. 6 indicates that changes are negligible, and mean friction coefficient is about 0.45.

Wear rate of different samples are compared in Fig. 8. It comes from this figure that wear rate of base metal is greater than other samples, and wear rate decreases as pass number increases. As pass number increases, distribution of nanoparticles in surface becomes more homogenized, and as it was stated before, hardness increases [7]. Based on Archad relation [21], wear rate decreases as hardness increases.

Furthermore, it comes from Fig. 8 that wear rate of processed samples using SiC particles do not differ from samples processed using Al_2O_3 particles, and both samples have nearly the same wear resistance.

3.3 Corrosion behavior

Figure 9 shows the polarization trends, for analysis by the Tafel extrapolarization method, of the four-pass FS-processed samples using SiC particles and the samples processed using Al_2O_3 particles. The cathodic polarization curves of the sample processed using Al_2O_3 particles show a very low current density in the potential range of concentration polarization,

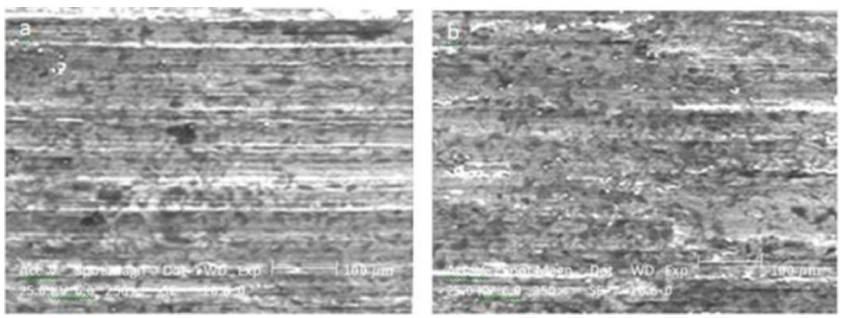

Fig. 7 SEM micrograph of worn surfaces relating to FS-processed samples for four passes (**a** relates to sample processed with SiC particles and **b** relates to sample processed with Al_2O_3 particles)

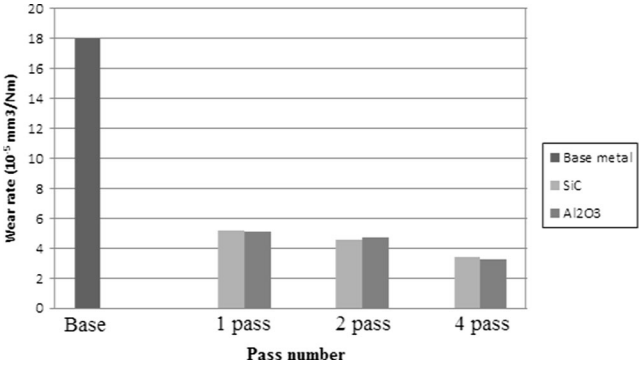

Fig. 8 Wear rate of FS-processed samples and base material

arising from a reduction in dissolved oxygen. The current density below the concentration polarization increased because of activation polarization as a result of the generation of atomic or molecular hydrogen. The anodic polarization curves at around OCP show low current densities. The behavior of the sample processed using SiC particles is similar to that of the sample processed using Al_2O_3 particles, although the corrosion potential is more positive (nobler). Table 3 compares the potentials, current densities, resistances, and rates of corrosion obtained by Tafel extrapolarization analyses of both the FS-processed specimens and the original AZ91 alloy [22]. The FS-processed specimens show an enhanced corrosion resistance, along with more noble characteristics and lower current densities, when compared with the original alloy in which any galvanic cell formation causes corrosion of that alloy. The reason for the improvement in corrosion properties might be the removal of local cell on the surface which could be formed by distribution of Mg particles on the surface layer. Furthermore, the release of residual stress by the annealing effect of stirring action during FSP can be the other reason. The results show the improved corrosion resistance of the FS-processed samples.

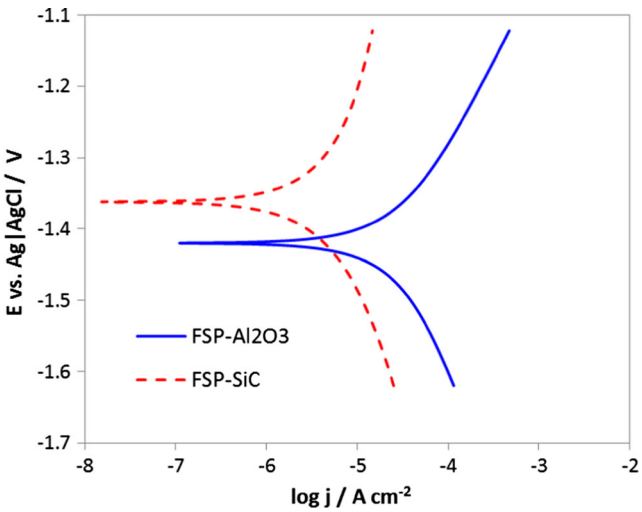

Fig. 9 The polarization trends of the four-pass FS-processed sample using SiC particles and of the processed sample using Al_2O_3 particles

Table 3 The potentials, current densities, resistances, and rates of corrosion obtained by Tafel extrapolarization analyses of both the FSPed specimens and the original AZ91 alloy

Specimen	i_{corr} ($A\,cm^{-2}$)	E_{corr} (V) vs Ag|AgCl	Corrosion rate (mm y^{-1})
FSP-Al2O3	3.16×10^{-5}	−1.42	0.72
FSP-SiC	1.41×10^{-5}	−1.36	0.32
Original AZ91 [19]	1.53×10^{-4}	−1.61	3.5

4 Conclusion

In the current research, surface composites were developed on the surface of AZ91 magnesium alloy by application of FSP. SiC and Al2O3 particles were embedded separately in the matrix during stirring, and two kinds of samples were developed. Different characteristics of developed materials were analyzed. Strength, ductility, hardness, tribologic characteristic, and corrosion resistance of FS-processed samples were studied. The results showed that mechanical and tribological properties of FS-processed samples were better than as-received material, and additionally, corrosion resistance of processed samples was higher. It was also concluded that

1. Increment of pass number up to four passes modifies the microstructure properly and accordingly mechanical, tribological properties enhance and corrosion resistance increases.
2. The samples FS-processed using SiC particles have better mechanical properties and corrosion resistance than samples processed using Al_2O_3 particles, although the wear rate of FS-processed samples was not significantly dependent to particle type.

References

1. Singh J, Lal H, Bala N (2013) Investigations on the wear behavior of friction stir processed magnesium based AZ91 alloy. Int J Mech Eng Robot Res 2:1–6
2. Asadi P, Faraji GH, Besharati MK (2010) Producing of AZ91/SiC composite by friction stir processing (FSP). Int J Adv Manuf Technol 51:247–260
3. Çam G (2011) Friction stir welded structural materials: beyond Al-alloys. Int Mater Rev 56:1–48
4. Mishra RS, Ma ZY (2005) Friction stir welding and processing. Mater Sci Eng R 50:1–78
5. Çam G, Mistikoglu S (2014) Recent development in friction stir welding of Al-alloys. J Mater Eng Perform 23:1936–1953
6. Uematsu Y, Tokaji K, Fujiwara K, Tozaki Y, Shibata H (2009) Fatigue behavior of cast magnesium alloy AZ91 microstructurally modified by friction stir processing. Fatigue Fract Eng Mater Struct 32:541–551

7. Dadaei M, Omidvar H, Bagheri B, Jehazi M, Abbasi M (2014) The effect of SiC/Al_2O_3 particles used during FSP on mechanical properties of AZ91 magnesium alloy. Int J Mater Res 105:369–374
8. Sterling CJ (2010) Effects of friction stir processing on the microstructure and mechanical properties of fusion welded 304 L stainless steel. Thesis, Brigham Young University, USA, M. Sc
9. Srinivasan A, Ajithkumar KK, Swaminathan J, Pillai UTS, Pai BC (2013) Creep behavior of AZ91 magnesium alloy. Procedia Eng 55: 109–113
10. Arora HS, Singh HS, Dhindaw BK (2012) Some observations on microstructural changes in a Mg-based AE42 alloy subjected to friction stir processing. Metall Mater Trans B43:92–108
11. Faraji G, Dastani O, Mousavi SAAA (2011) Effect of process parameters on microstructure and micro-hardness of AZ91/Al2O3 surface composite produced by FSP. J Mater Eng Perform 20:1583–1590
12. Karthikeyan L, Senthilkumar VS, Padmanabhan KA (2010) On the role of process variables in the friction stir processing of cast aluminum A319 alloy. Mater Des 31:761–771
13. 13 ASTM-E8M (2003) Standard test methods of tension testing of metallic materials [metric], Annual Book of ASTM Standards, Vol. 3.01, American Society for Testing and Materials, USA (2003).
14. Dadaei M (2011) Investigation into the effects of FSP on different properties of AZ91 magnesium alloy. Thesis, Department of Materials Engineering, Islamic Azad University, Tehran, Iran, M. Sc
15. 15 ASTM-G99 (2003) Standard test method for wear testing with a pin-on-disk apparatus, Vol. 3.02, American Society for Testing and Materials, USA
16. Callister WD (2007) Materials science and engineering: an introduction. Wiley, USA
17. Ma ZY, Pilchak AL, Juhas MC, Williams JC (2008) Microstructural refinement and property enhancement of cast light alloys via friction stir processing. Scripta Mater 58:361–366
18. Tutunchilar S, Haghpanahi M, Besharati Givi MK, Asadi P, Bahemmat P (2012) Simulation of material flow in friction stir processing of a cast Al-Si alloy. Mater Des 40:415–426
19. Naderi M, Abbasi M, Saeed-Akbari A (2013) Enhanced mechanical properties of a hot-stamped advanced high-strength steel via tempering treatment. Metall Mater Trans A44:1852–1861
20. Sarkar AD (1976) Wear of metals. Elsevier, USA
21. Archard JF (1953) Contact and rubbing of flat surfaces. J Appl Phy 24:981–995
22. Shi Z, Liu M, Atrens A (2010) Measurement of the corrosion rate of magnesium alloys using Tafel extrapolation. Corr Sci 52:579–588